Truck Load Distribution Behavior of the Bridge Street Bridge, Southfield, Michigan

Nabil F. Grace, Ph.D., P.E.
Professor and Chairman
Civil Engineering Department
Lawrence Technological University
Southfield, Michigan

Richard B. Nacey, P.E.
Senior Project Engineer
Hubbell, Roth & Clark, Inc.
Bloomfield Hills, Michigan

John J. Roller, P.E., S.E.
Principal Structural Engineer
Construction Technology
Laboratories, Inc.
Skokie, Illinois

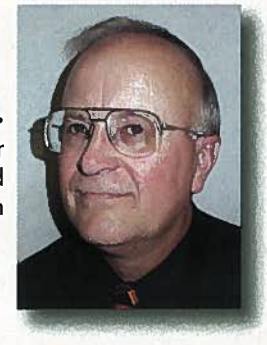

Wayne Bonus, P.E.
Administrative Engineer
City of Southfield
Southfield, Michigan

Frederick C. Navarre, P.E.
Chief Structural Engineer
Hubbell, Roth & Clark, Inc.
Bloomfield Hills, Michigan

This paper presents the major results and details from a structural load test performed on Structure B of the Bridge Street Bridge Deployment Project in Southfield, Michigan. Structure B is the first prestressed concrete bridge in the United States to be almost entirely reinforced with carbon fiber reinforced polymer. The measured strains and deflections from various bridge span load configurations were analyzed for evaluating load distribution behavior. In addition, data from a laboratory test of a full-scale prototype double-tee test beam conducted prior to bridge construction were compared with data obtained from the field load test of Structure B. Static loads were applied to each of the three spans of Structure B using loaded dump trucks to generate specific positive lane bending moments. Based on the results from the static load test of Structure B, it is concluded that the three spans of the bridge exhibit similar load distribution behavior. As determined from the measured strain response in the beams, the actual distribution of the applied loads within each span in general conforms with the provisions contained in the AASHTO Specifications.

As a result of extensive research efforts, fibrous composite materials are now being used in the construction of innovative civil engineering structures throughout the world.[1] These structures include bridge beams, girders, and slabs containing special reinforcing elements.[2-3] One notable example of this emerging technology in North America is the Bridge Street Bridge Deployment Project in Southfield, Michigan.[4]

This project includes the first prestressed concrete bridge in the United States to be almost entirely reinforced with carbon fiber reinforced polymer (CFRP). The findings of several research investigations conducted at Lawrence Technological University, Southfield, Michigan, and funded by the National Science Foundation, formulated the technical basis for the implementation of this technology.[5-10]

The Bridge Street Bridge Deployment Project (see Figs. 1a and 1b, and Fig. 2) consists of two parallel, independent bridges (Structures A and B) over the Rouge River in the City of Southfield, Michigan. Both structures were designed to accommodate two traffic lanes and incorporated three 68.9 ft (21 m) long, 27.9 ft (8.5 m) wide spans skewed at an angle of 15 degrees relative to the substructure. Structure A incorporates five equally spaced conventional prestressed AASHTO I-beams in each of the three spans.

Structure B consists of 12 double-tee beams (four beams per span), each incorporating internal pretensioned Leadline™ tendons and external post-tensioned carbon fiber composite cable

Fig. 1a. Southward view of Bridge Street Bridge, Southfield, Michigan. CFRP structure, Structure B, is on the right.

(CFCC™) tendons. Fig. 3 shows a section through the superstructure. Specific construction details related to the project can be found elsewhere.[4] This paper presents the major findings and details related to a field load test conducted on Structure B after completion of construction.

BRIDGE DESIGN DETAILS

Hubbell, Roth & Clark, Inc. (HRC), Bloomfield Hills, Michigan, was responsible for the design of the Bridge Street Bridge Deployment Project. Bridge Structures A and B were designed for two traffic lanes using provisions of both the AASHTO Standard Specifications for Highway Bridges[11] and LRFD Bridge Design Specifications.[12] As shown in Fig. 3, the superstructure dead loads for Structure B included the double-tee beams, composite CFRP-reinforced concrete topping, surfacing mixture, pedestrian sidewalk, concrete barrier, and the bridge parapet and railing. Live load design was based on Michigan MS-23 (AASHTO HS25) truck loading.

Fig 1b. Side view of Structure B.

During the design phase, values for the live load distribution factor were investigated using provisions of both sets of AASHTO bridge specifications. The typical derivation of the LRFD live load distribution factor is based on the longitudinal stiffness parameter, K_g, calculated using the moment of inertia of the full composite section of each double-tee beam, resulting here in a value of approximately 0.63 lanes per beam. Likewise, distribution factor calculations performed using the provisions of Section 3.23.4 of the AASHTO Standard Specifications resulted in a similar value of approximately 0.64 lanes per beam.

Within the provisions of Section 4.6.2.2 of the AASHTO LRFD Specifications, HRC considered the moment of inertia of the beam webs alone to cal-

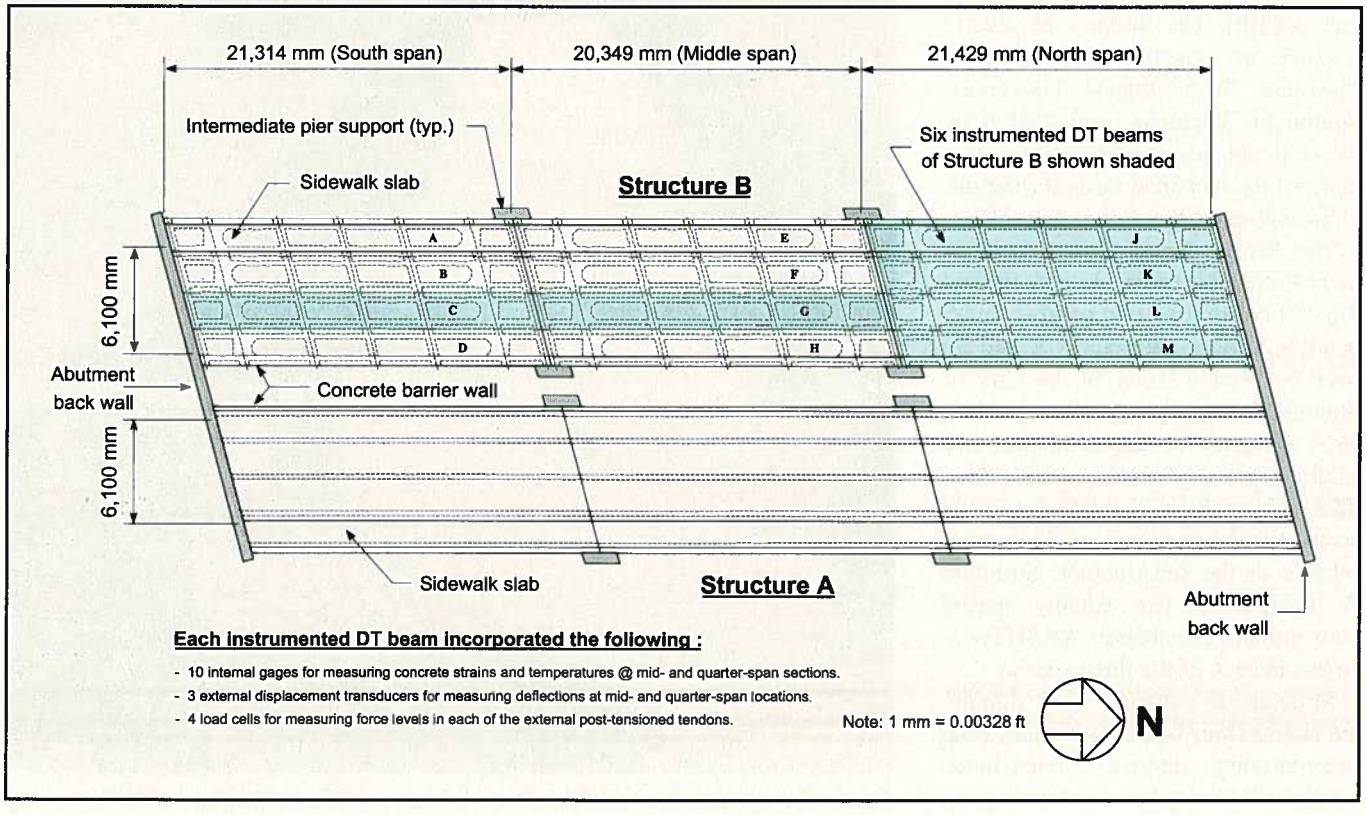

Fig. 2. Plan view of Bridge Street Bridge.

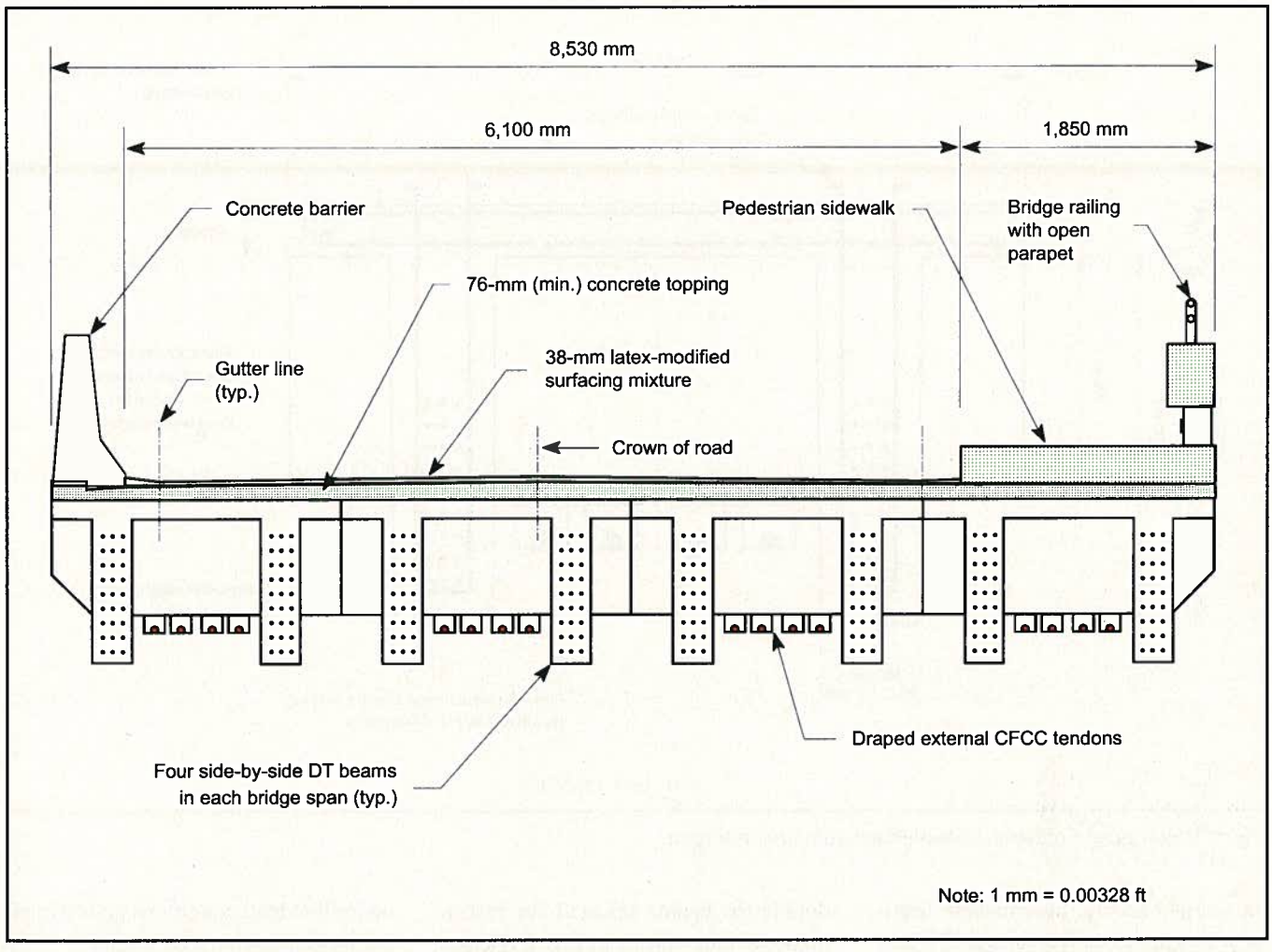

Fig. 3. Section view through superstructure of Structure B looking south.

culate an alternate value of the longitudinal stiffness parameter, K_g, resulting in a distribution factor of 0.81 lanes per beam. The nominal ratio of this alternative distribution factor was noted to be about 1.3. Calculations showing the design live load distribution factors are shown in Appendix A.

The Michigan MS-23 truck loading resulted in a maximum live load per lane plus impact bending moment equal to 1496 kip-ft (2028 kN-m). Since Structure B was to be the first bridge to incorporate prestressed concrete beams made using CFRP exclusively as the primary reinforcement, a conservative approach was appropriate to establish the design live load. Therefore, each double-tee beam was designed for a live load plus impact ($LL+I$) moment equal to 1197 kip-ft (1622 kN-m), or approximately 1.3 times the typical design value.

For most design conditions, the full composite beam section is typically used in the determination of the longitudinal beam stiffness. Therefore, for evaluating the load distribution behavior of Structure B, comparisons are made with the live load distribution factor equal to 0.6 lanes per beam. As indicated in Appendix A, the live load distribution factors calculated using the various AASHTO provisions ranged from 0.63 (LRFD Specifications) to 0.64 (Standard Specifications).

CONSTRUCTION

Prestressed Systems Incorporated in Windsor, Ontario, Canada, fabricated 12 double-tee beams for Structure B of the Bridge Street Bridge Deployment Project. The double-tee beams were each cast with seven diaphragms to enhance transverse stiffness, house transverse post-tensioned CFRP tendons, and provide deviator-bearing elements for the draped longitudinal post-tensioned CFRP tendons. A cross-sectional view of a typical double-tee beam cut near midspan is shown in Fig. 4. Each beam incorporated 60 internal 0.39 in. (10 mm) diameter Leadline™ CFRP pretensioning tendons (30 in each beam stem).

In addition to the Leadline tendons, each beam also incorporated four draped longitudinal external 1.58 in. (40 mm) diameter post-tensioning CFCC™ tendons. Other longitudinal and transverse non-prestressed reinforcement in the beam flange and diaphragms were also made of CFRP. The epoxy-coated stainless steel stirrups used for shear reinforcement in each beam stem were the only internal metallic reinforcement components incorporated in the beams.

After fabrication in Canada, the 12 double-tee beams were transported to the bridge site. Each of the three bridge spans of Structure B incorporated four double-tee beams erected side-by-side, as shown in Figs. 2 and 3. Each double-

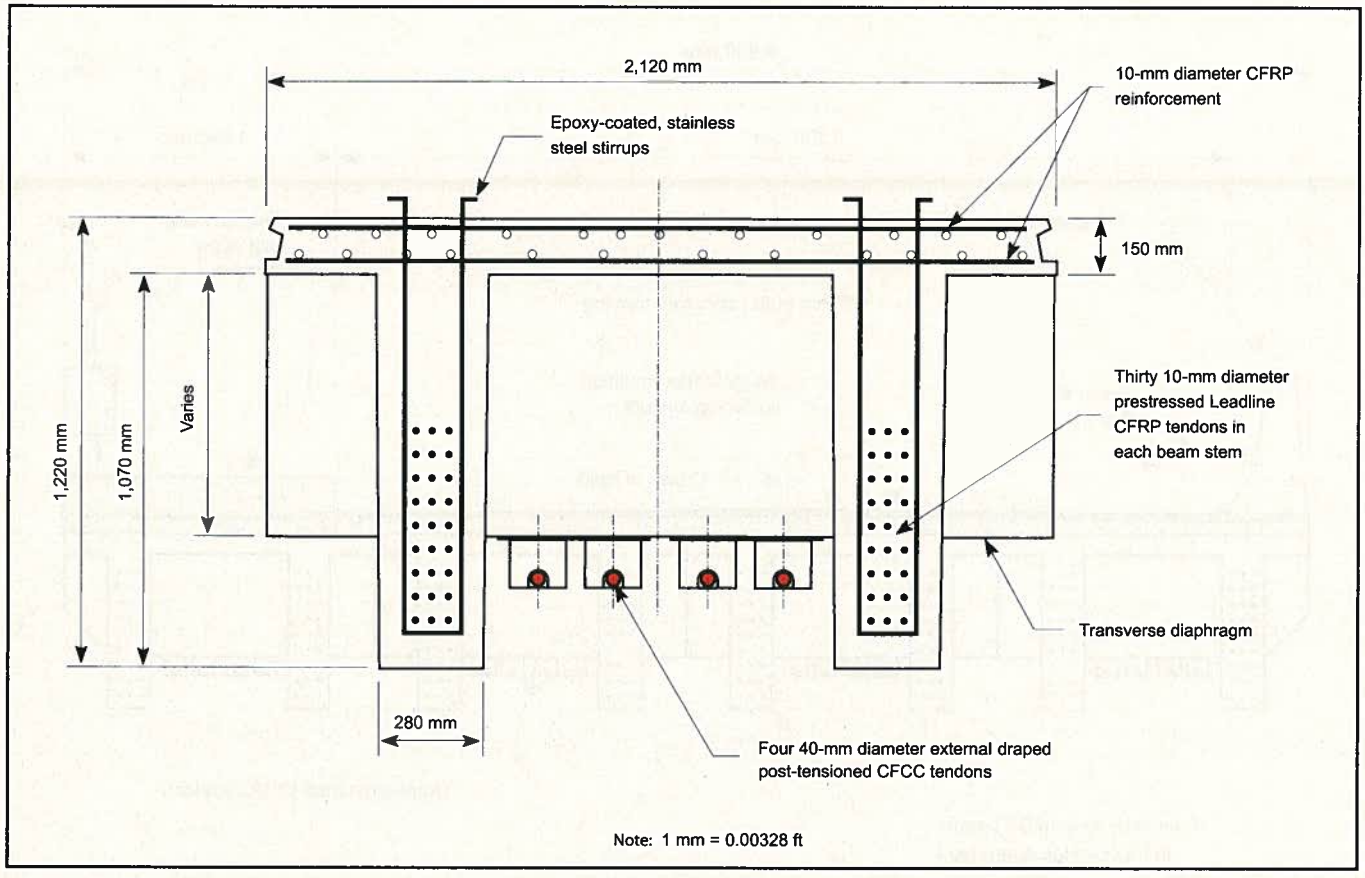

Fig. 4. Cross section of typical double-tee beam near midspan.

tee beam had five intermediate transverse diaphragms (D2 through D6) and two end transverse diaphragms (D1 and D7). Additional CFCC tendons were installed in the transverse diaphragms and were used to post-tension the four beams in each span together.

After erection, a 3 in. (76 mm) minimum thick concrete topping reinforced with NEFMAC™ grids was placed over each span. The concrete topping was discontinuous over the supports and anchored to the double-tee beams by the hooked stirrup ends that protruded from the top flange. A 1.5 in. (38 mm) thick latex-modified surfacing mixture was added over the concrete topping within the 20 ft (6.1 m) wide clear roadway bounded by the pedestrian sidewalk along the west side of the bridge and concrete barrier on the east side.

INSTRUMENTATION

During fabrication, six of the 12 double-tee beams for Structure B were instrumented with various sensors to measure concrete strains, beam deflections, and force levels in the external CFCC post-tensioned tendons. The six double-tee beams selected for instrumentation are shown in Fig. 2 (Beams C, G, J, K, L, and M).

Once the double-tee beams were erected at the bridge site, additional sensors were installed throughout Structure B during the various stages of construction. All sensors were connected to a dedicated on-site data acquisition system used to monitor the long-term behavior of the bridge. Instrumentation of the bridge beams and installation of the data acquisition system was performed by Construction Technology Laboratories, Inc. (CTL), of Skokie, Illinois.

INSPECTION AND LOAD TESTING

After construction was complete, CTL conducted a visual inspection and static load test. Visual inspection was done to document the size and location of any concrete cracks visible to the unaided eye both before and after the load test. The objective of the static load test was to evaluate structural performance under live load conditions approximating design service load levels.

Visual Inspection

Before conducting the static load test, an initial visual inspection of Structure B was conducted to document the as-built condition. The visual inspection included the top and underside of the superstructure. With the exception of the beam diaphragms that provided anchorage for the external longitudinal post-tensioning tendons (D2 and D6), there were no structural cracks found during the inspection. After the static load test was completed, there were no apparent new cracks and no discernable difference observed in the existing diaphragm cracks.

Static Load Test Details

After the initial visual inspection was completed, a static load test was conducted on November 28, 2001. Static loads were applied to each span (individually) using two identical tandem rear-axle dump trucks provided by the City of Southfield. The specified empty

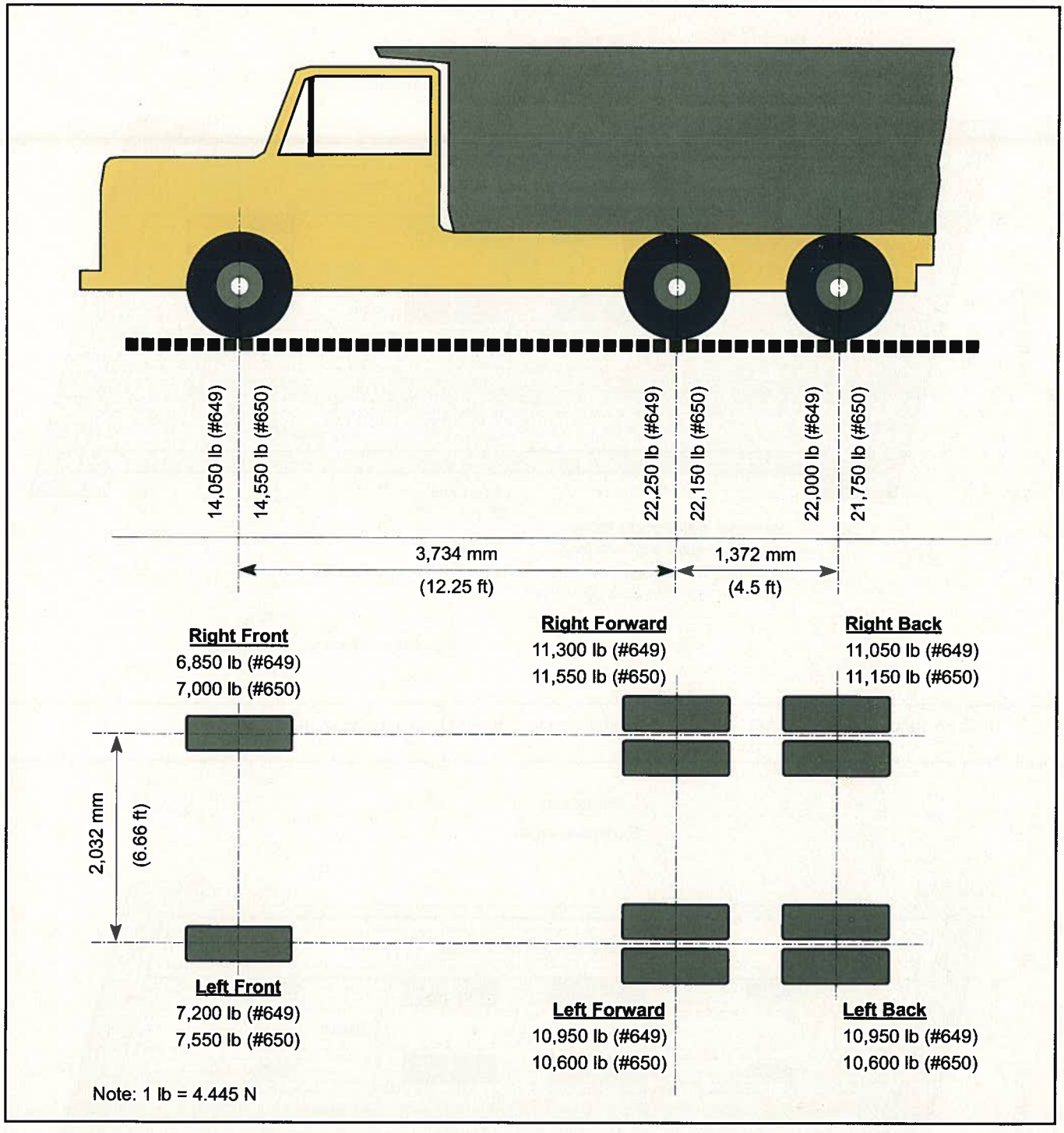

Fig. 5. Dump truck configuration and measured wheel loads.

gross weight of each dump truck was 26,700 lb (119 kN). Prior to the test, each dump truck was filled with granular material to achieve a total target vehicle weight of 58,000 lb (258 kN).

After filling, the actual weight of each truck was measured by the chief weigh master for the Road Commission for Oakland County. During this exercise, portable scales, accurate to within ±1 percent of reading, were used to measure the load distributed to each of the three axles. Details and measured axle loads for both dump trucks (Truck Nos. 649 and 650) are shown in Fig. 5. The filled weights of both trucks were within 450 lb (2.0 kN) of the 58,000 lb (258 kN) target weight.

The load test consisted of four different stages of loading. Each loading stage consisted of positioning the two dump trucks back to back in one lane near midspan, as shown in Fig. 6. The first two load stages consisted of positioning

Fig. 6. Typical truck orientation used for each load stage.

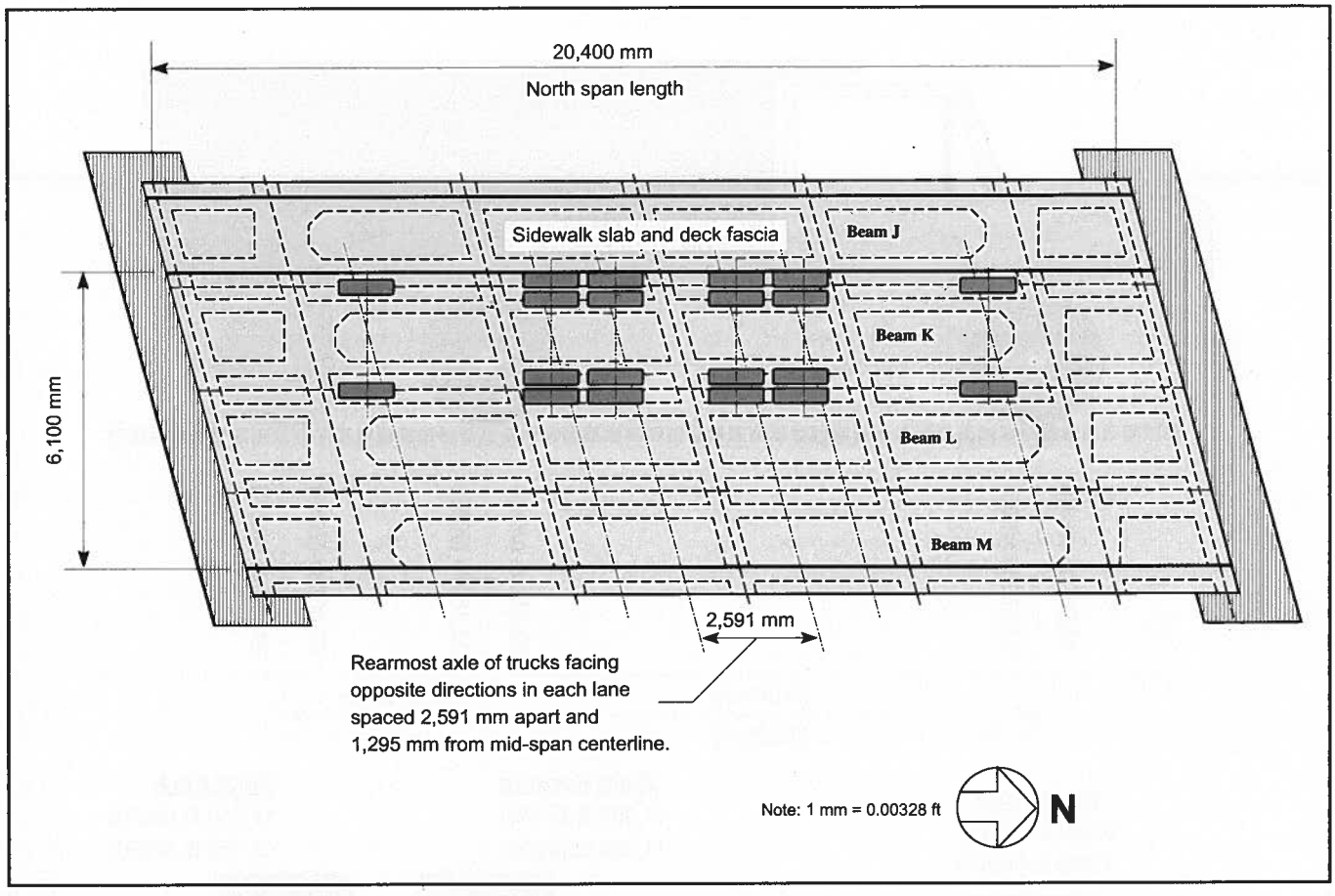

Fig. 7. Truck positions for Load Stage 1: Maximum positive moment in west lane of north span.

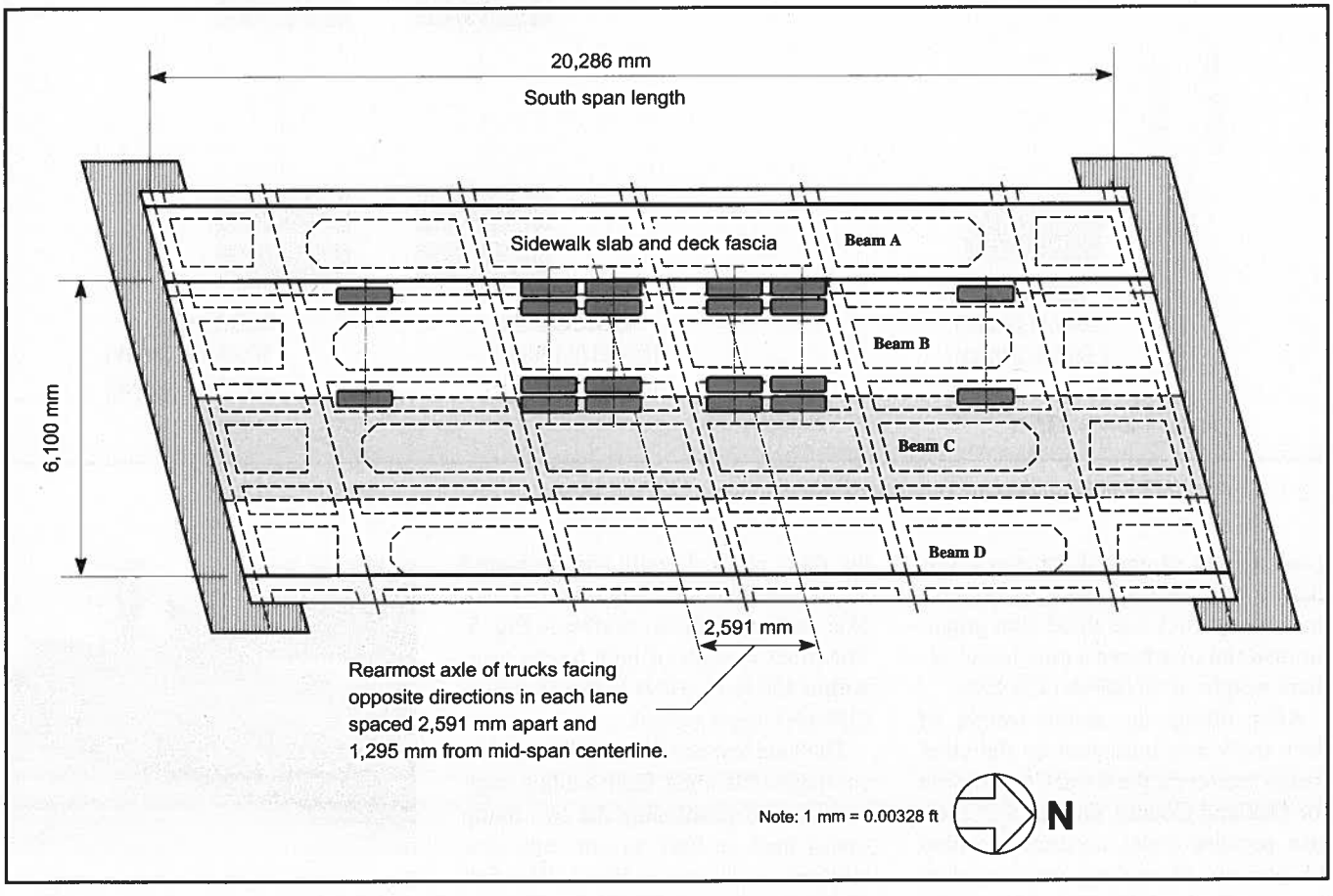

Fig. 8. Truck positions for Load Stage 2: Maximum positive moment in west lane of south span.

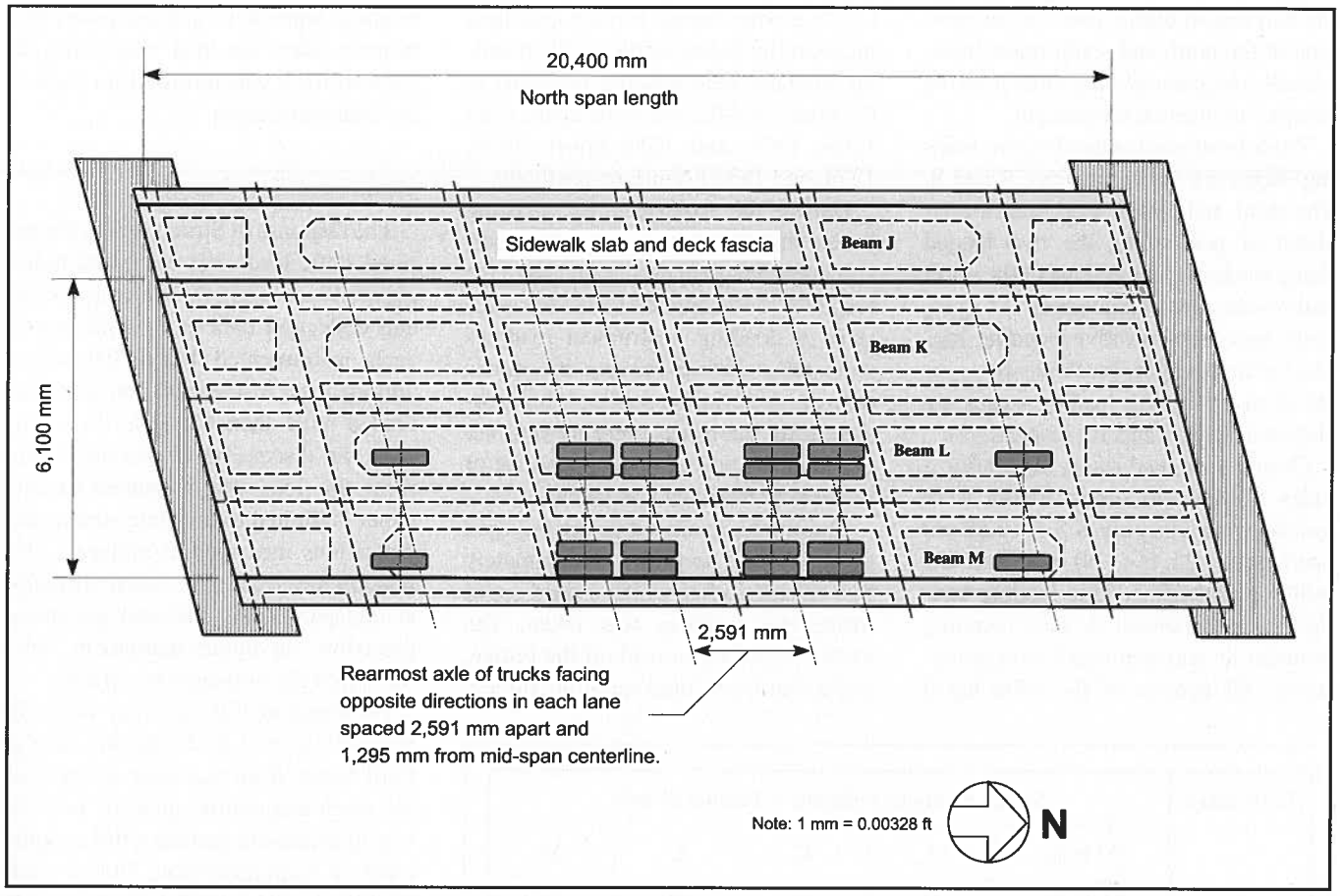

Fig. 9. Truck positions for Load Stage 3: Maximum positive moment in east lane of north span.

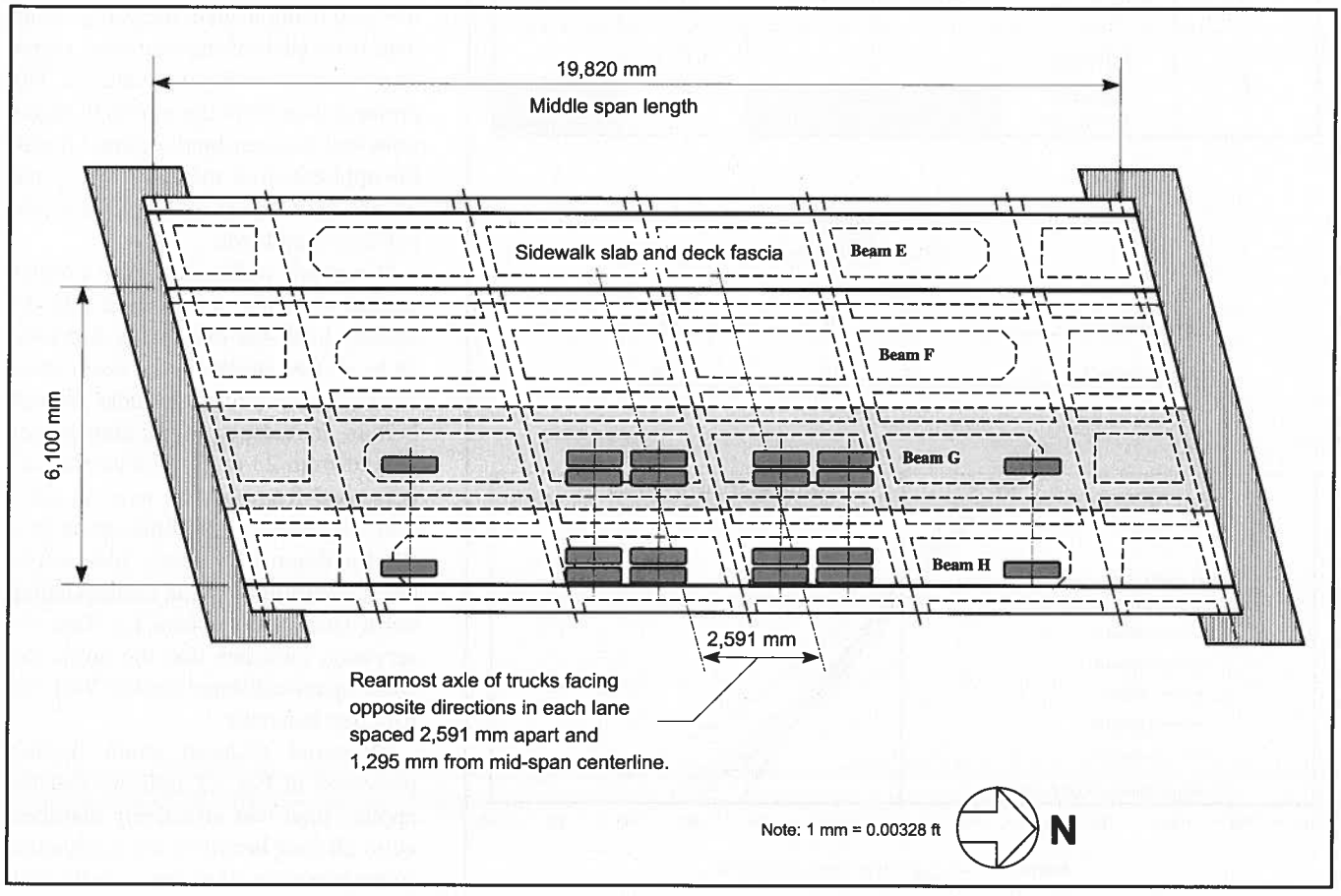

Fig. 10. Truck positions for Load Stage 4: Maximum positive moment in east lane of middle span.

the two loaded dump trucks in the west lane of the north and south spans (individually) to generate maximum positive bending moment at mid-length.

Truck positions for the first two loading stages are shown in Figs. 7 and 8. The third and fourth load stages consisted of positioning the two loaded dump trucks in the east lane of the north and middle spans (individually) to generate maximum positive bending moment at mid-length. Truck positions for the third and fourth loading stages are shown in Figs. 9 and 10, respectively.

During each load stage, the rearmost axles of the two dump trucks were spaced approximately 8.5 ft (2.59 m) apart and 4.25 ft (1.30 m) from the midspan centerline. This loading configuration produced a lane bending moment at midspan equal to approximately 90 percent of the 1496 kip-ft (2028 kN-m) design service live load moment (including impact). The resulting midspan lane bending moments in the north, middle, and south spans were 1364, 1309, and 1355 kip-ft (1850, 1774, and 1836 kN-m), respectively.

During the load test, the existing bridge instrumentation and data acquisition system were used to measure the response to the applied loads. For each stage of loading, instrument readings were taken before moving the trucks onto the span (initial reading). Immediately after the trucks were moved into the required positions, a second set of instrument readings was taken.

The trucks remained in the required positions for a period of approximately five minutes, after which a third set of instrument readings was taken. The trucks were then moved off the bridge, and a fourth and final set of instrument readings were taken approximately five minutes after the load was removed. This protocol was followed for each of the four load stages.

Load Stage	Strain location: midspan @ bottom of web				
1	DT beam	J	K	L	M
	Concrete strain, $\mu\varepsilon$	45	34	30	23
	% Total strain	34.1	25.8	22.7	17.4
2	DT beam			C	
	Concrete strain, $\mu\varepsilon$			29	

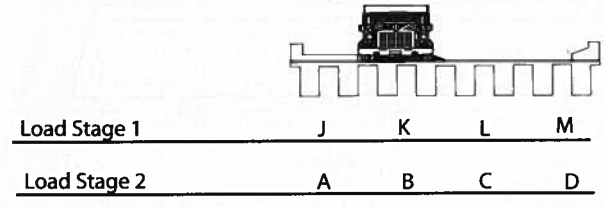

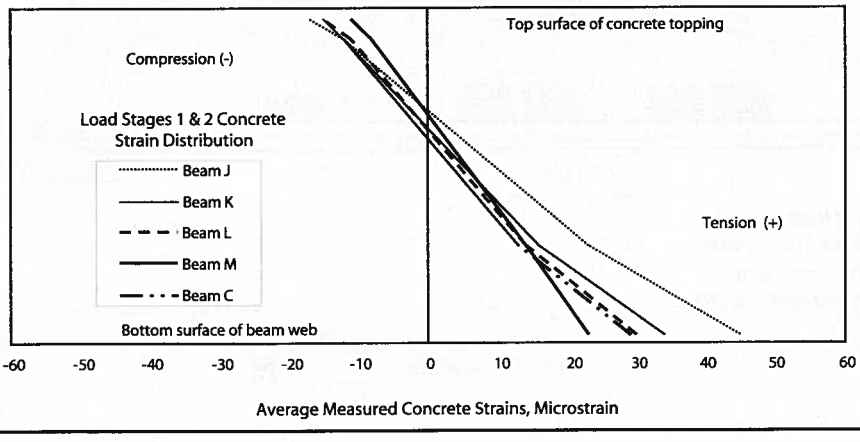

Fig. 11. Load Stages 1 and 2: Measured responses for Beams J to M and C.

Static Load Test Results

The response of Structure B to the applied static loads was evaluated based primarily on measured concrete strains and deflection data at the midspan of each instrumented beam. Therefore, although the instrumentation array included more than 450 individual sensors, the discussion of measured data from the load test presented in this paper is limited to concrete strains and deflections measured at midspan. Deflection measurements, taken manually at midspan during the load test using precision surveying equipment, corroborated the measured strain data.

As noted in Fig. 2, every beam in the north span (J, K, L, and M) and the third beam from the west in each of the south and middle spans (C and G), was fabricated to include a full compliment of instrumentation. During each load stage, measured data were collected for the instrumented beams in the span being loaded. Measured strain data from each of the four load stages are presented in Figs. 11 and 12. The reported data from the four load stages represent the measured response due to the application of the truck loads, and do not include the effects of the pre-existing dead loads.

Measured midspan strain profiles presented in Fig. 11 indicate that the applied load was effectively distributed to all four beams in the north span. Average measured strains near the web bottom at midspan of the four beams ranged from 23 to 45 microstrain, and decreased from west to east. In addition, the measured midspan strain profile for Beam C is nearly identical to the strain profile for the corresponding north span beam (Beam L). This observation indicates that the north and south spans exhibited similar load distribution behavior.

Measured midspan strain profiles presented in Fig. 12 indicate that the applied load was effectively distributed to all four beams in the north span. Average measured strains near the web bottom at midspan of the four beams

in the north span ranged from 15 to 51 microstrain, decreased from east to west, and were consistent with the corresponding measured deflections. Measured strain data from this load stage were similar to the data from Load Stage 1. The additional stiffness contributed by the sidewalk installed over Beam J most likely accounted for the slight variation occurring between the peak strains measured during Load Stages 1 and 3.

It is also observed that the measured midspan strain profile for Beam G (see Fig. 12) is almost identical to the strain profile for the corresponding north span beam (Beam L). This observation indicates that the north and middle spans also exhibited similar load distribution behavior.

LOAD DISTRIBUTION BEHAVIOR

The load distribution behavior of Structure B was evaluated by comparing the measured strain response during the truck load test to the load distribution factors derived from the AASHTO design provisions. In addition, data from a structural load test performed on a single prototype double-tee beam incorporating details identical to those of the bridge beams was used for making further comparisons with the truck load test data from Structure B.

Measured Strain Response During Truck Load Test

The measured data from Load Stages 1 to 4 indicate that all three spans exhibit very similar load distribution behavior. As shown in Fig. 13, the maximum measured strain response during the load test was obtained when the trucks were positioned in the east lane of Structure B (Load Stage 3). It is very likely that the east lane loading condition represented the worst-case scenario for bending stresses to occur due to the greater eccentricity of the load from the center of the bridge and the absence of the sidewalk along this side of the bridge.

A comparison of the average measured concrete strains in the web bottom of Beams J to M during Load Stages 1 and 3 can be used to provide an indication of the load distribution in the north bridge span. Such a comparison is shown in Fig. 14 for the combined effects of Load Stages 1 and 3. Based on the magnitude of the average measured bottom web strains, the cumulative percentages of the applied lane loads distributed to each of the four beams in the north span (Beams J, K, L, and M) would be 46.3, 43.7, 51.2, and 58.9 percent, respectively.

Using this rationale, it can be theorized that no more than 60 percent of the total lane live load would be distributed to any individual beam. This percentage is in good agreement with the AASHTO distribution factor of 0.60 lanes per beam resulting from the condition where the full composite section is used in the calculation of longitudinal stiffness.

Comparison of Measured Strains in Structure B and Prototype Beam

The truck configuration used during the load test of Structure B produced a lane bending moment at midspan equal to approximately 90 percent of the design service moment ($LL+I$). This percentage corresponds to an applied lane bending moment of approximately 1346 kip-ft (1825 kN-m). Prior to fabrication of the bridge beams for Structure B, a single prototype double-tee beam was fabricated by the precaster and shipped to CTL for testing.[13,14]

During fabrication, strain gauge instrumentation was installed by CTL at three different sections along the length of the prototype double-tee beam, at the locations shown in Fig. 15. The configuration of the strain gauge instrumentation installed in the prototype

Load Stage	Strain location: midspan @ bottom of web				
3	DT beam	J	K	L	M
	Concrete strain, $\mu\varepsilon$	15	22	35	51
	% Total strain	12.2	17.9	28.5	41.5
4	DT beam			G	
	Concrete strain, $\mu\varepsilon$			36	

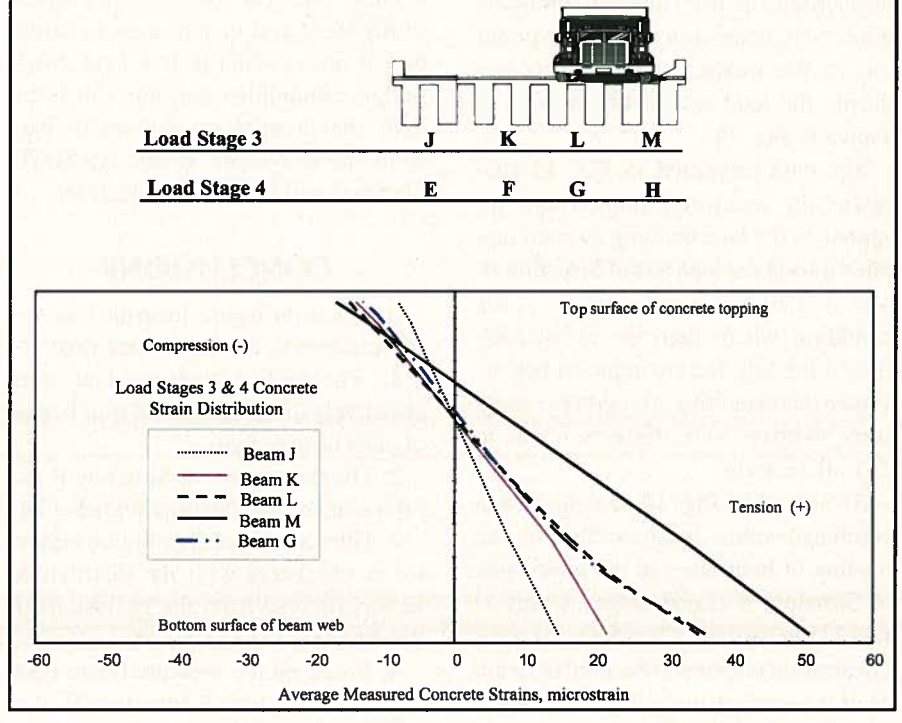

Fig. 12. Load Stages 3 and 4: Measured responses for Beams J to M and G.

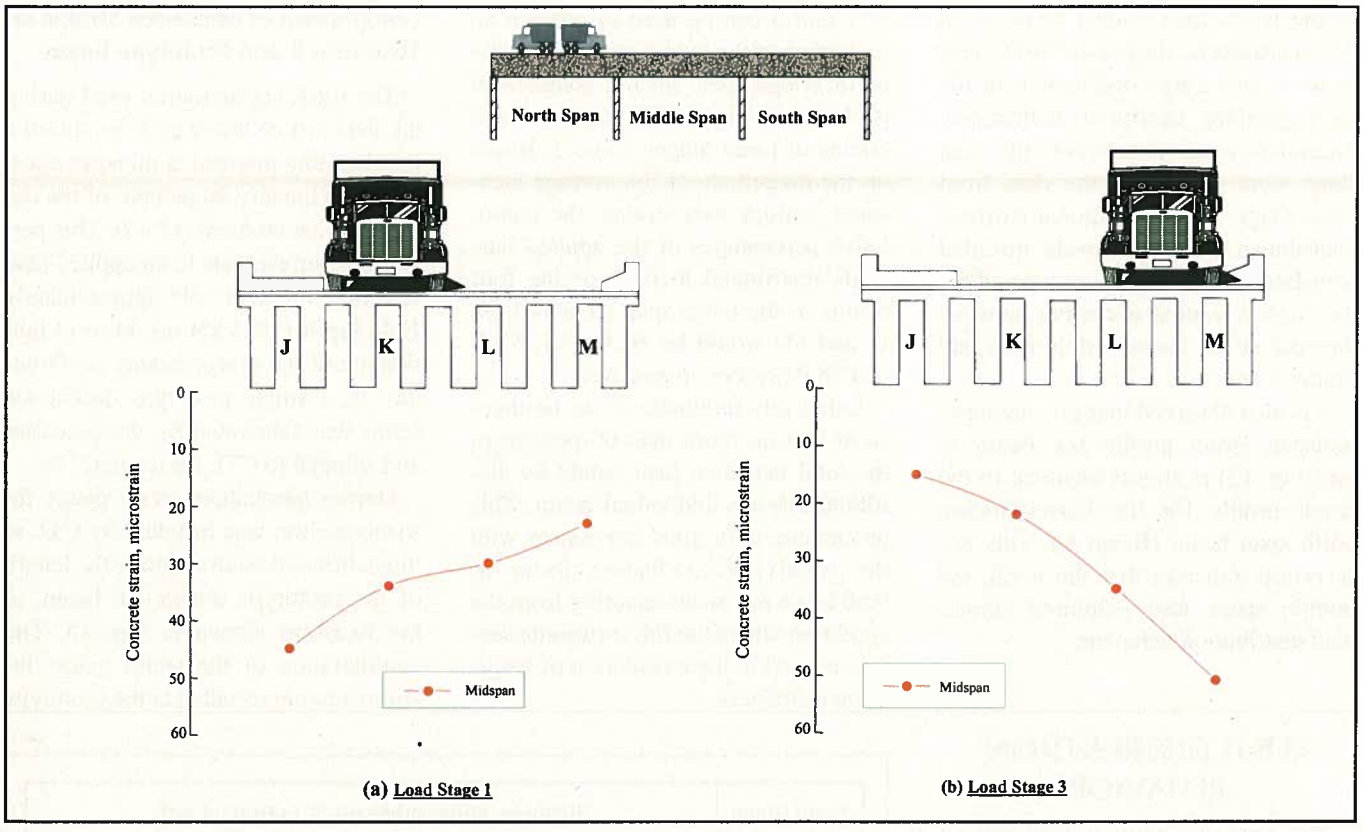

Fig. 13. Average measured strain at bottom of double-tee web, north span.

beam was identical to that used in the instrumented double-tee beams incorporated in Structure B.

The prototype beam was tested with the concrete topping applied, but without any transverse post-tensioning applied through diaphragms. The measured response from the prototype double-tee beam at a load corresponding to the moment applied per lane during the load test of Structure B is shown in Fig. 15.

The data presented in Fig. 15 represent the measured single-beam response to the lane bending moment applied during the load test of Structure B. The single-beam response reflects the condition where there is no distribution of the lane load to adjacent beams. Under this condition, the average measured bottom web strain is equal to 251 microstrain.

As shown in Fig. 14, the maximum combined strain response due to the loading of both lanes of the north span of Structure B (Load Stages 1 plus 3) was 74 microstrain. Therefore, the combined strain response measured in Beam M of the north span during Load Stages 1 and 3 was equal to approximately 30 percent of the response measured in the prototype double-tee beam.

Based on this result, it is apparent that the longitudinal stiffness of the completed bridge structure is considerably greater than the sum of the stiffness contribution from the four beams in each span. The overall effectiveness of the structural system used in Structure B has resulted in live load distribution capabilities that are consistent with the distribution factors derived from the provisions of the AASHTO Standard and LRFD Specifications.

CONCLUSIONS

Based on the results from the load test of Structure B, it is concluded that:

1. The applied loads per lane were effectively distributed to all four beams of each bridge span.

2. The three spans of Structure B exhibit similar load distribution behavior.

3. The actual load distribution behavior is consistent with the distribution factors derived from the provisions of the AASHTO Specifications.

4. Based on the measured data from the truck load test of Structure B, it is concluded that the provisions of the AASHTO Standard or LRFD Specifications can be used to predict the load distribution behavior of bridge superstructure configurations similar to that of Structure B.

ACKNOWLEDGMENTS

The success of this project is due to the energy and talent of many people, each of whom played a significant role. These include various researchers, designers, manufacturers, suppliers, and builders. The project benefited from the congressional support of Michigan Representatives Joseph Knollenberg and Sander Levin. The site construction was funded in the 1998 fiscal year through the Federal Highway Administration (FHWA) as one of the TEA-21 High Priority Projects. Further funding for instrumentation and monitoring was provided under the Innovative Bridge Research and Construction Program of TEA-21.

The Bridge Street Industrial Park Subdivision property owners approved the formation of a Special Assessment District, created by the City of Southfield, which contributed to the funding of the project. In addition, the project

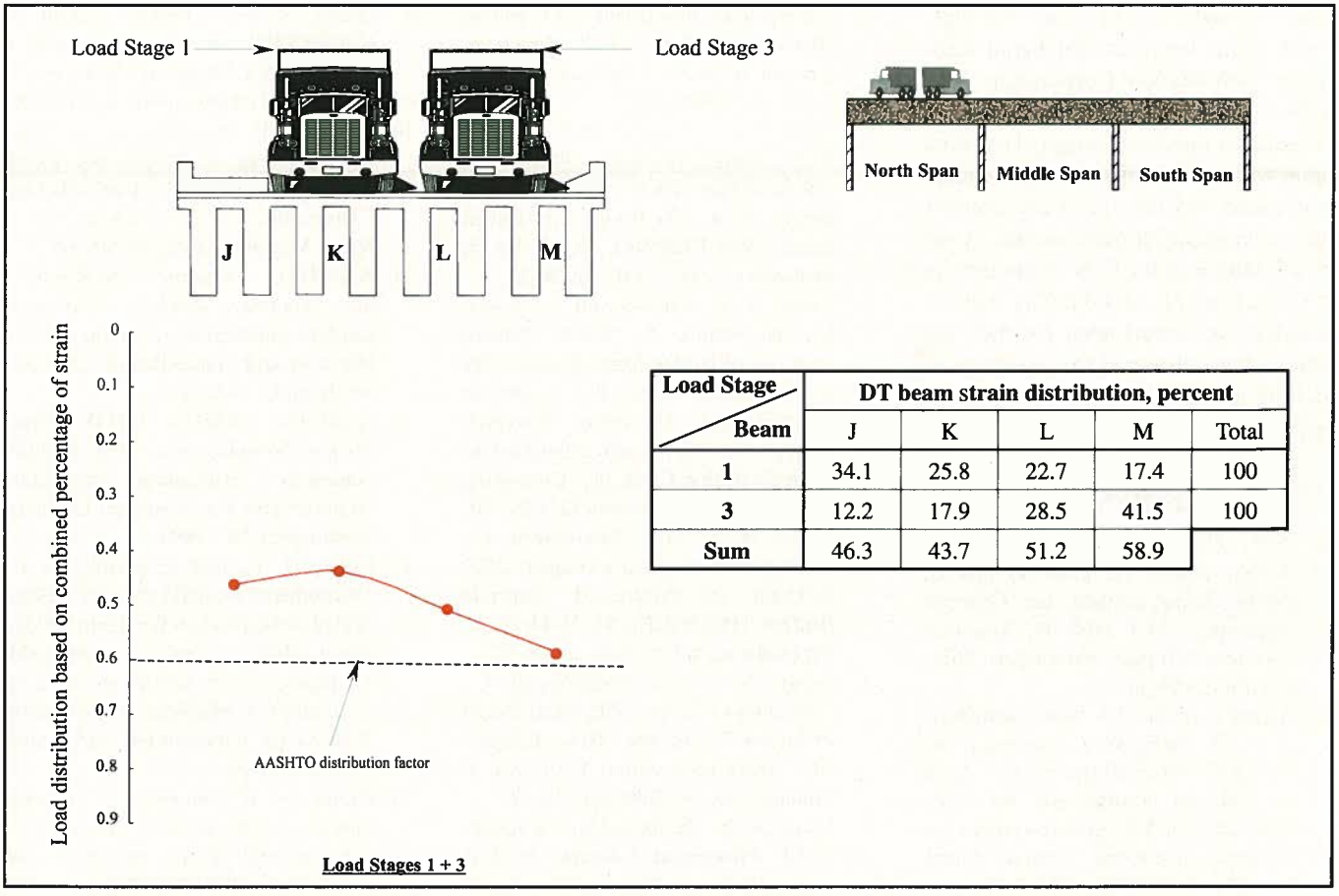

Load Stage / Beam	DT beam strain distribution, percent				
	J	K	L	M	Total
1	34.1	25.8	22.7	17.4	100
3	12.2	17.9	28.5	41.5	100
Sum	46.3	43.7	51.2	58.9	

Fig. 14. Load distribution based on combined percentage of strain, north span.

DT test beam	Measured concrete strain, $\mu\varepsilon$					
	Location	Midspan				Measured deflection, mm
		East	Middle	West	Ave	
	Topping	-139	-223	-211	-191	12.49
	Flange	-131	-128	-140	-133	
	C.G. of tendons	115		113	114	
	Bottom of web	258		243	251	

Note: 1 in. = 25.4 mm

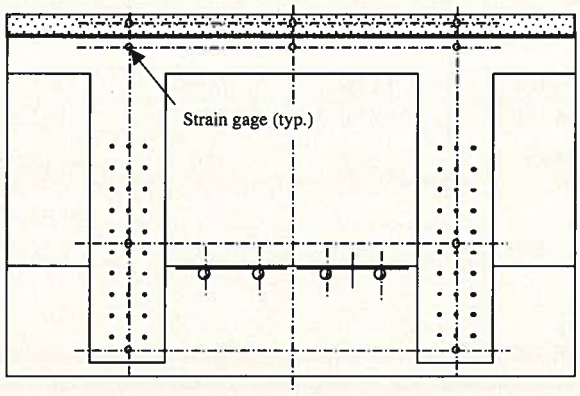

Concrete Strain gage locations at midspan

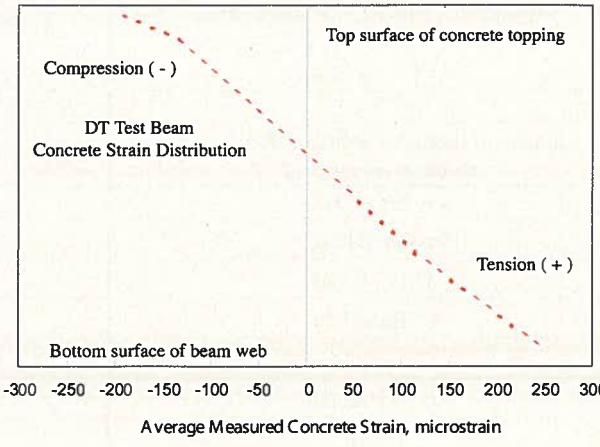

Fig. 15. Measured double-tee test beam response at 90 percent of design lane moment ($LL+I$).

was awarded a Michigan Strategic Fund Grant from the Michigan Economic Development Corporation.

Furthermore, the National Science Foundation funded the original research upon which the project design concept was based and the analytical analysis presented in earlier publications. Finally, the Mayor of the City of Southfield, the City Council, and the City Administration are commended for their vision of the future and their courage to venture into this exciting new technology in bridge construction.

REFERENCES

1. ACI Committee 440, "State-of-the-Art Report on Fiber Reinforced Plastic Reinforcement for Concrete Structures," ACI 440R-96, American Concrete Institute, Farmington Hills, MI, 1996, 153 pp.
2. Rizkalla, S. H., "A New Generation of Civil Engineering Structures and Bridges," Proceedings of the Third International Symposium on Non-Metallic (FRPRC) Reinforcement for Concrete Structures, Sapporo, Japan, V. 1, October 1997, pp. 113-128.
3. Fam, A. Z., Rizkalla, S. H., and Tadros, G., "Behavior of CFRP Prestressing and Shear Reinforcements for Concrete Highway Bridges," *ACI Structural Journal*, V. 94, No. 1, January-February 1997, pp. 77-86.
4. Grace, N. F., Navarre, F. C., Nacey, R. B., Bonus, W., and Collavino, L., "Design-Construction of Bridge Street Bridge – First CFRP Bridge in the United States," PCI JOURNAL, V. 47, No. 5, September-October 2002, pp. 20-35.
5. Grace, N. F., Abdel-Sayed, G., Sakla, S., and Wahba, J., "Finite Element Analysis of Bridge Street Bridge, City of Southfield, Michigan," Lawrence Technological University Research Project No. 36, Report Submitted to Hubbell, Roth & Clark, Inc., Consulting Engineers, 1997, Bloomfield Hills, MI.
6. Grace, N. F., and Abdel-Sayed, G., "Behavior of Externally Draped CFRP Tendons in Prestressed Concrete Bridges," PCI JOURNAL, V. 43, No. 5, September-October 1998, pp. 88-101.
7. Grace, N. F., and Abdel-Sayed, G., "Behavior of Carbon Fiber Reinforced Prestressed Concrete Skew Bridge," *ACI Structural Journal*, V. 97, No. 1, January-February 2000, pp. 26-34.
8. Grace, N. F., "Response of Continuous CFRP Prestressed Concrete Bridges Under Static and Repeated Loadings," PCI JOURNAL, V. 45, No. 6, November-December 2000, pp. 84-102.
9. Grace, N. F., "Transfer Length of CFRP/CFCC Strands for Double-T Girders," PCI JOURNAL, V. 45, No. 5, September-October 2000, pp. 110-126.
10. Grace, N. F., Enomoto, T., and Yagi, K., "Behavior of CFCC and CFRP Leadline Prestressing Systems in Bridge Construction," PCI JOURNAL, V. 47, No. 3, May-June 2002, pp. 90-103.
11. AASHTO, *Standard Specifications for Highway Bridges*, Sixteenth Edition, American Association of State Highway and Transportation Officials, Washington, DC, 1996.
12. AASHTO, *AASHTO LRFD Bridge Design Specifications*, First Edition, American Association of State Highway and Transportation Officials, Washington, DC, 1994.
13. Roller, J. J., and Elremaily, A. F., "Instrumentation and Structural Testing of Full-Scale Double-Tee Beam, Bridge Street Bridge, City of Southfield, Michigan," Final Report to the City of Southfield, Michigan, Construction Technology Laboratories, Inc., April 13, 2001, 46 pp.
14. Grace, N. F., Enomoto, T., Abdel-Sayed, G., Yagi, K., and Collavino, L., "Experimental Study and Analysis of a Full-Scale CFRP/CFCC Double-Tee Bridge Beam," PCI JOURNAL, V. 48, No. 4, July-August 2003, pp. 120-139.

Table A1. Evaluation of load fraction based on AASHTO Standard Specifications.[11]

Parameter	Stems		Flange		Sum
	1	2	Bottom	Top	
Width, b (in.)	42	42	84	84	—
Thickness, t (in.)	11.5	11.5	6	3	—
J components (Eq. A1.5) (in.^{4})	20,615	20,615	6758	739	48,727
Modulus of elasticity ratio, n	1.17	1.17	1.17	1.0	—
Cross-sectional area, A (sq in.)	483	483	504	252	1722
nA (sq in.)	565.11	565.11	589.68	252	1971.9
Distance to centoid of cross-sectional components from extreme bottom fiber, y (in.)	21	21	45	49.5	—
nAy (in.^{3})	11,867.31	11,867.31	26,535.6	12,474	62,744.22
Distance to centroid of whole section from extreme bottom fiber, $\bar{y}$ (in.)	31.82	31.82	31.82	31.82	—
$d = \lvert y - \bar{y} \rvert$ (in.)	10.82	10.82	13.18	17.68	—
Ad^2 (in.^{3})	66,158.78	66,158.78	102,434.73	78,770.77	313,523
Moment of inertia of sectional component about its own axis, I_o	83,071.17	83,071.17	1769	189	168,100.34
$I = \Sigma(I_o + Ad^2)$	—				481,623.34
Poisson's ratio, ν	0.16				
K (Eq. A1.4)	3.386				
C (Eq. A1.3)	1.450 < 5				
N_L	2				
D (Eq. A1.2)	5.456				
S (ft)	7.0				
Load fraction, S/D (Eq. A1.1)	1.283				

APPENDIX A – LOAD DISTRIBUTION FACTORS

The typical derivations of load distribution factors based on AASHTO Standard Specifications (Section 3.23.4.3)[11] and AASHTO LRFD Specifications (Section 4.6.2.2)[12] are presented below:

(a) AASHTO Standard Specifications, Section 3.23.4.3

From Eq. (3-11):

$$\text{Load fraction} = \frac{S}{D} \quad \text{(A1.1)}$$

where

$$D = (5.75 - 0.5N_L) + 0.7N_L\,(1 - 0.2C)^2 \quad \text{(A1.2)}$$

$$C = K\left(\frac{W}{L}\right) \quad \text{(A1.3)}$$

$$K = \left[(1+\nu)\frac{I}{J}\right]^{0.5} \quad \text{(A1.4)}$$

$$J = \Sigma\left[\frac{bt^3}{3}\left(1 - 0.63\,\frac{t}{b}\right)\right], \text{ where } b > t \quad \text{(A1.5)}$$

in which

S = spacing between beams (ft)
N_L = number of lanes
W = overall width of bridge
I = moment of inertia of cross section
J = Saint-Venant torsion constant
ν = Poisson's ratio

Evaluation of the various parameters to calculate the load fraction is presented in Table A1. It should be noted that Eq. A1.1 would provide a distribution factor per wheel load, per double-tee beam.

ASD distribution factors: ASD distribution factors (*S/D*) per truck load, per double-tee beam for interior and fascia beam can be expressed in terms of AASHTO distribution factors (per wheel load, per double-tee beam).

(i) ASD distribution factor (*S/D*) for interior beam

$$= 0.5 \times (S/D) \text{ (per Eq. A1.1)} \quad \text{(A1.6)}$$

(ii) ASD distribution factor for fascia beam (exterior beam) can be obtained from Eqs. A1.7 and A1.8, as given below:

$$\frac{S}{D} = \frac{S}{4 + 0.25S} \quad \text{(A1.7)}$$

S/D for exterior beams, per truck load, per double-tee beam

$$= 0.5 \times (S/D) \text{ (obtained from Eq. A1.7)} \quad \text{(A1.8)}$$

(b) AASHTO LRFD Specifications, Section 4.6.2.2.2b

It should be noted that for typical cross sections (Table 4.6.2.2.1.1), distribution factors for two or more design-loaded lanes could be determined using Eqs. A1.9 and A1.10:

$$\text{Factor} = 0.075 + \left(\frac{S}{9.5}\right)^{0.6}\left(\frac{S}{L}\right)^{0.2}\left[\frac{K_g}{12\,Lt_s^3}\right]^{0.1} \quad \text{(A1.9)}$$

$$K_g = n\,(I + Ae_g^2) \quad \text{(A1.10)}$$

where

K_g = longitudinal stiffness parameter (in.^{4})
n = ratio of modulus of elasticity of girder to slab
t_s = slab thickness (in.)
S = center-to-center spacing between adjacent beams (ft)
L = span of beam (ft)

Note that the term $(I + Ae_g^2)$ is the moment of inertia of the section about its axis passing through the centroid of the section.

The values of the distribution factor parameters considering (1) the center-to-center spacing of the composite beam as a whole and (2) the spacing between the webs of the double-tee beam are presented in Table A2.

Table A2. Computation of load distribution factors for the double-tee (DT) beam.

Load distribution factor based on spacing between composite beams as a whole		**Load distribution factor based on spacing between webs of the DT beam**	
Parameter	**Value**	**Parameter**	**Value**
n	1.17	n	1.17
Flange top thickness, in.	3	Web width, b, in.	11.5
Flange bottom thickness, in.	6	Web height, h, in.	42
Distance to centroid of flange from extreme compression fiber, in.	4.653	Web cross-sectional area, nA, sq in.	565.11
nI_o, in.^{4}	481,623.34	Moment of inertia of web, nI, in.^{4}	83,071.1
nA, sq in.	1971.9	Flange thickness, t_s, in.	9
e_g, in.	14.527	e_g, in.	25.347
K_g, in.^{4} (Eq. A1.10)	897,760.8	K_g, in.^{4}	446,137.6
S, ft	7	L, ft	66.93
L, ft	66.93	S, ft	4
t_s, in.	9	t_s, in.	9
LRFD distribution factor, per truck load, per DT beam (Eq. A1.9)	0.627	LRFD distribution factor, per truck load, per web, Eq. A1.9	0.404
		LRFD distribution factor, per truck load, per DT beam	0.808